J|A|C|S COMMUNICATIONS

Published on Web 07/24/2009

Experimental and Computational Evaluation of Forces Directing the Association of Transmembrane Helices

Yao Zhang,[†] Daniel W. Kulp,[‡] James D. Lear,[‡] and William F. DeGrado*[,†,‡]

Department of Chemistry, University of Pennsylvania, 231 South 34th Street, Philadelphia, Pennsylvania 19104, and Department of Biochemistry and Biophysics, University of Pennsylvania, 1009 Stellar Chance Laboratories, 36th and Hamilton Walk, Philadelphia, Pennsylvania 19104

Received June 7, 2009; E-mail: wdegrado@mail.med.upenn.edu

While our understanding of the features stabilizing the structures of water-soluble proteins has reached an advanced state, a parallel understanding of membrane protein folding is only beginning to emerge.[1] Previous work on water-soluble proteins suggests that the burial of hydrophobic residues plays a crucial role for folding.[2,3] Similarly, the replacement of large apolar side chains with smaller residues in the interior of membrane proteins results in introduction of cavities with a concomitant loss in thermodynamic stability.[4] From this perspective, the packing of large apolar side chains can stabilize the folded structure of the membrane protein. By contrast, statistical,[5−9] computational,[10−12] and experimental[10,11,13] studies have demonstrated that small side chains, such as Ser, Ala, and Gly, occur frequently at the helix−helix interface of membrane proteins, suggesting that the appropriate packing of these residues might provide an even stronger driving force for transmembrane (TM) helix association. We therefore compared the effects of packing large vs small apolar side chains, using a simple transmembrane TM helical dimer.

Coiled-coils, such as the leucine zipper from GCN4,[2,3] have a repetitive 7-residue repeat providing a conceptually simple system for studying side chain packing. By convention, the residues at the "*a*" and "*d*" positions of the heptad pack in the core of a coiled-coil. The stability of water-soluble coiled-coils scales with the size and hydrophobicity of the side chains at the "*a*" position increasing over the series Gly < Ala <Val < Ile.[3,14] Interestingly here we show just the opposite rank for MS1, a membrane-soluble version of a leucine zipper.

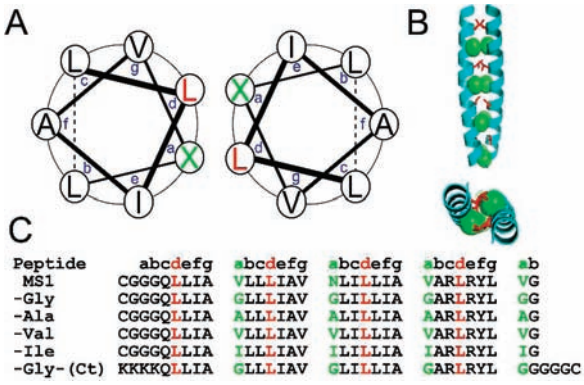

Figure 1. Helical wheel (A), computational model showing side and top view (B), and sequence of MS1 variants (C). MS1, -Gly, -Ala, -Val, and -Ile are N-terminally Cys-modified. -Gly-(Ct) is C-terminally Cys-modified. The variable "*a*" positions are shown in green, and the Leu at "*d*" in red. All peptides had an N-terminal acetyl group.

MS1 is a membrane-soluble derivative of GCN4-P1, rendered lipophilic by converting its exposed polar side chains to apolar residues, while maintaining the core residues constant.[15] We synthesized a series of MS1 variants in which each of the four "*a*" positions was varied to Gly, Ala, Val, and Ile (Figure 1). Each of these peptides is predominantly helical in a dodecylphosphocholine (DPC) micelle as determined by circular dichroism over the entire range of peptide/DPC ratios studied here (Figure S1). Their assembly was first examined in DPC micelles by analytical ultracentrifugation (AUC) under conditions where the density of the solution is adjusted by addition of D_2O to eliminate the mass contribution of DPC. The degree of association of membrane peptides in micelles depends on the concentration of peptide in the micelle phase as reflected in the peptide/detergent ratio. Over all experimentally accessible peptide/detergent ratios, MS1-Gly was fully dimeric, MS1-Ala adopted a monomer−dimer equilibrium, and the most hydrophobic peptides, MS1-Val and MS1-Ile, were predominantly monomeric (Table 1, Figure S2). This ranking is precisely the opposite of that found in water-soluble structures.

Table 1. Association States of MS1 Variants Determined by AUC

	observed MW	monomer MW	ratio[a]
MS1-Gly	6300 ± 600	3214.4	2.0 ± 0.2
MS1-Ala	5600 ± 200	3270.5	1.7 ± 0.1
MS1-Val	3200 ± 300	3359.3	1.0 ± 0.1
MS1-Ile	3100 ± 500	3438.8	1.0 ± 0.2

[a] Ratio = observed MW/monomer MW.

To explore the association strength of the MS1 variants we employed the method of equilibrium thiol/disulfide exchange,[16] which is well-suited for examining weak interactions. The N-terminus was modified with a flexible three-glycine linker followed by a cysteine (Figure 1C). After peptides were incorporated into detergent micelles, redox buffer was added to bring the system to the following equilibrium (Scheme 1).

Scheme 1

$$2\mathrm{Mon_{SH}} \underset{K_{dim}}{\rightleftharpoons} \mathrm{Dim_{SH}} \overset{GSSG}{\underset{2GSH}{\rightleftharpoons}} \mathrm{Dim_{SS}} \qquad K_{dim} = \frac{[\mathrm{Dim_{SH}}]}{[\mathrm{Mon_{SH}}]^2} \qquad K_{ox} = \frac{[\mathrm{Dim_{SS}}][\mathrm{GSH}]^2}{[\mathrm{Dim_{SH}}][\mathrm{GSSG}]}$$

The two steps in Scheme 1 are linked but depend differently on the peptide concentration: the dimerization step (K_{dim}) is a reversible bimolecular association reaction that depends on the reduced monomer concentration (Mon_{SH}); the subsequent oxidation step (K_{ox}) is also reversible but independent of the concentration of the peptide and dependent on the ratio of oxidized (GSSG) to reduced glutathione (GSH). Using this function we fit curves to obtain the

[†] Department of Chemistry.
[‡] Department of Biochemistry and Biophysics.

Table 2. pK_{dim} and pK_{ox} Obtained from Analysis of Data in Figure 2A[a]

	pK_{dim}	pK_{ox}	ΔG_{dim} (kcal/mol dimer)
MS1	−2.6	1.5	−3.6
-Gly	−3.0	2.6	−4.1
-Ala	−1.6	1.2	−2.2
-Val	0.9	−0.8	1.2
-Ile	1.9	−2.0	2.6

[a] The error is estimated to be approximately 10% based on the error in experimental concentrations of the reduced and oxidized peptides.

parameters K_{dim} and K_{ox} for each MS1 variant (Table 2; Figures S3, 2A). Comparison of ΔG_{dim} for each variant suggests that the amino acid in the "*a*" position aids the association of membrane helices in increasing order of Gly > Ala > Val > Ile, in good agreement with the AUC data. Clearly, the association of the helices increases as the size of the core position side chain decreases.

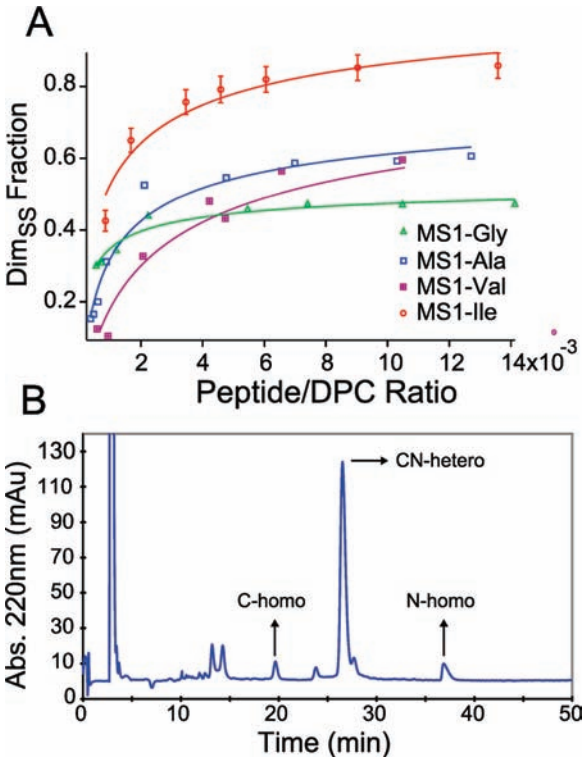

Figure 2. (A) Analysis of the fraction of cross-linked dimer as a function of peptide/DPC ratios for each MS1/variant. The theoretical curve describes the least-squares fit to Scheme 1 (Table 2). The standard errors in the experimental points are similar for each peptide and are indicated for MS1-Ile (others are not so shown for clarity). (B) HPLC chromatogram after redox equilibration of the C-terminal and N-terminal Cys-modified MS1-Gly mixture indicates that MS1-Gly prefers an antiparallel orientation. The other peaks are glutathione adducts.

Interestingly, as the size of the side chain at the "*a*" position decreases, the ease of disulfide formation (reflected in K_{ox}) becomes less favorable. This was surprising, given that the peptides have a Gly3 linker between the helical ends and the Cys. As long as the helices pack in a parallel manner, the flexibility of the linker should easily accommodate any subtle differences in helix-packing (two Cys-Gly3 linkers could extend up to ∼20 Å, while interhelical distances in dimers vary by only ∼0−4 Å). Thus, we considered the possibility that MS1-Gly prefers to assume an antiparallel orientation. In this case, association of Mon_{SH} would remain favorable, but the oxidation step would require unfavorable intramolecular rearrangement of the antiparallel dimer, $Dim_{(anti)SH}$, to the parallel, $Dim_{(parallel)SH}$, to allow disulfide formation, because of the need to shift the equilibrium from one favoring antiparallel to parallel dimers upon disulfide formation (Scheme 2). This effect can be seen in Figure 2A, in which the fraction of disulfide formation levels off at relatively low [Peptide]/[DPC] for MS1-Gly (reflecting high dimerization affinity). However, under these redox conditions, the curve for MS1-Gly extrapolates to a low fraction disulfide at high [Peptide]/[DPC], indicating that disulfide formation is thermodynamically less favorable than for the other variants.

Scheme 2

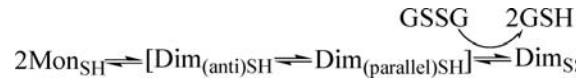

To test this hypothesis, we synthesized a C-terminally Cys-modified peptide (Figure 1C, -Gly-(Ct)), which was mixed in equal amounts with N-terminally Cys-labeled MS1-Gly under reversible redox conditions. If MS1-Gly has the same preference to form parallel dimers as antiparallel dimers, then a ratio of 1:1:2 (N-terminal homodimer/C-terminal homodimer/heterodimer) is expected. However, the experimental ratio is 1:1:14, indicating that MS1-Gly strongly prefers to form antiparallel dimers (Figure 2B).

To probe further the orientation of MS1-Gly and the other variants, the peptides with N-terminal Cys residues were individually air-oxidized to force an N-terminal cross-link (Figures 3, S4). Under these conditions peptides with a strong tendency to form antiparallel dimers might be expected to oligomerize as shown in Figure 3C. To avoid the precipitation of polymers during centrifugation, we performed the experiment on samples that were ∼(75 ± 5)% oxidized. The ratio between the computed molecular weight from a single-species fit and the computed monomeric molecular weight roughly reflects the degree of oligomerization (Table S1). The computed ratio for MS1-Gly is 6.9, supporting the expectation that MS1-Gly prefers an antiparallel orientation. MS1-Ala has a ratio of ∼3, in agreement with the conclusion that this peptide prefers to form weak, antiparallel dimers. The ratio for MS1-Val and MS1-Ile is less than 2, again consistent with the suggestion that they form even weaker parallel dimers. Thus, as the side chains in the core positions become smaller, the helices prefer to form an antiparallel orientation.

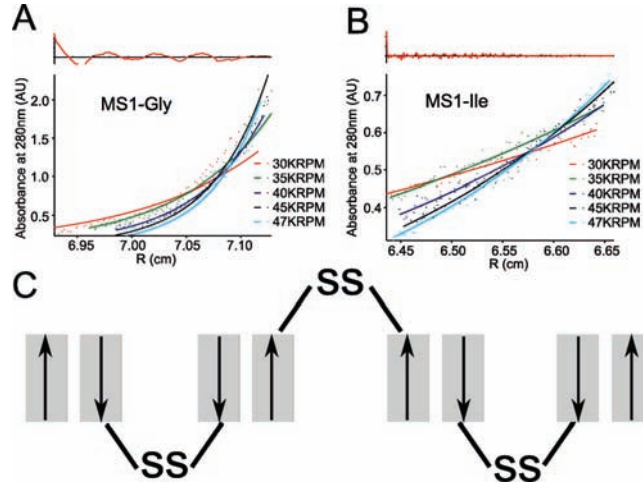

Figure 3. Analytical ultracentrifugation of ∼(75 ± 5)% disulfide-bonded MS1-Gly (A) and MS1-Ile (B). The greater degree of curvature in panel A vs B is indicative of greater oligomerization. (C) Oligomerization of MS1-Gly and MS1-Ala via formation of antiparallel dimers.

To investigate the energetic and structural mechanisms behind these observations, we built parallel and antiparallel computational models for the MS1 variants. While long simulations in bilayers would be essential to fully evaluate the relative energetic contributions from helix−helix, helix−lipid, and lipid−lipid components, successful models[17] and designs[18] of transmembrane proteins have been achieved by probing helix−helix packing interactions alone, using a much simpler gas phase potential energy function. For each sequence, the conformational space available to parallel and antiparallel two-stranded coiled-coils (Figure 4A) was globally searched using a molecular mechanics force field to compute the difference in energy between the homodimer versus the isolated monomers as described in the supplement. The resulting energy landscapes (Figure 4B) have global minima corresponding to structures in which the variable "*a*" position projects toward the core of the structure as in Figure 1B.

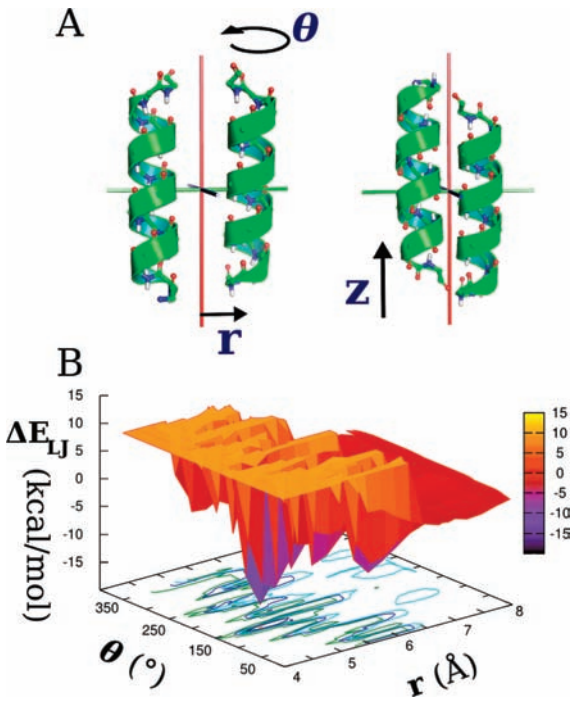

Figure 4. (A) Sampling Crick parameters for parallel (r, θ) and antiparallel (r, θ, z-translation) dimers. (B) Energy landscape showing the difference in computed Leonard−Jones energy E_{LJ} (for the dimer versus two monomers) of MS1-Gly in a parallel orientation. The minimum in the surface has a helical phase (θ) of 154°, allowing packing of the Gly residues at the helix/helix interface as in Figure 1B.

The calculations are in remarkable agreement with experiment, given the stark simplicity of the calculations. The global minimum energy conformations (GMEC) for MS1-Gly and MS1-Ala correspond to antiparallel structures, which also allow the closest approach of the helices (Table S2). By contrast, the GMEC conformations for MS1-Val and MS1-Ile correspond to parallel structures. To gain insight into the interactions responsible for these structures, some of the energetic components were investigated, specifically the change in Leonard−Jones energy (ΔE_{LJ}, approximating the van der Waals component) and the electrostatic term associated with interactions between the partial charges of the main chain atoms at the interface (ΔE_{bb}). The values of ΔE_{LJ} for the GMEC structures correlate with the experimental ranking (ΔG_{dim}), in terms of both overall energetics of association and the preference for parallel versus antiparallel structures (Table 3). Moreover, although the magnitude of ΔE_{bb} depends on the electrostatic treatment employed in these calculations, there is a clear trend toward greater stabilization of the antiparallel structure as the residues at the "*a*" position (and hence the interhelical separation) become smaller.

Table 3. Energetic Contributions for Minima in Energy Landscape[a]

peptide	parallel		anti-parallel		Δ(orientation)[b]	
MS1-	ΔE_{LJ}	ΔE_{bb}	ΔE_{LJ}	ΔE_{bb}	$\Delta\Delta E_{LJ}$	$\Delta\Delta E_{bb}$
Gly	−23.5	2.8	**−38.0**	**−1.4**	−14.6	−4.2
Ala	−31.8	1.8	**−36.1**	**−0.9**	−4.3	−2.7
Val	**−35.2**	**0.8**	−26.2	−1.0	9.1	−1.8
Ile	**−32.3**	**0.4**	−28.8	−0.1	3.5	−0.5

[a] Units are kcal/mol based on the CHARMM force field. Values in bold give the values of ΔE_{LJ} and ΔE_{bb} associated with the GMECs. [b] Δ(orientation) represents the energetic difference between the global minimum for the antiparallel vs parallel orientations.

These studies together with other studies of MS1 variants[10] show that small residues at TM helix−helix interfaces allow helices to come into close contact, concomitantly increasing their van der Waals interactions.[7,19] Thus, they are in agreement with previous studies highlighting the importance of van der Waals interaction,[4] while also demonstrating the important role that small residues can play in allowing particularly efficient packing to occur. Finally, we show that close interhelical distances associated with packing of small side chains can additionally facilitate interhelical electrostatic interactions between the partial charges of backbone atoms.

Acknowledgment. We acknowledge support from NIH Grant GM60610 and helpful discussions with Lidia Cristian, Paul Billings, Alessandro Senes, Ivan Korendovych, and Gevorg Grigoryan.

Supporting Information Available: Experimental and computational procedures, CD spectra, AUC data, computational data, and the full list of authors for all references. This material is available free of charge via the Internet at http://pubs.acs.org.

References

(1) DeGrado, W. F. *Protein Sci.* **2003**, *12*, 647–65.
(2) O'Shea, E. K. *Science* **1991**, *254*, 539–44.
(3) Acharya, A. *Biochemistry* **2006**, *45*, 11324–32.
(4) Faham, S. *J. Mol. Biol.* **2004**, *335*, 297–305.
(5) Walters, R. F. *Proc. Natl. Acad. Sci. U.S.A.* **2006**, *103*, 13658–63.
(6) Eilers, M. *Biophys. J.* **2002**, *82*, 2720–36.
(7) Liu, W. *J. Mol. Biol.* **2004**, *337*, 713–29.
(8) Senes, A. *J. Mol. Biol.* **2000**, *296*, 921–36.
(9) Adamian, L. *J. Mol. Biol.* **2001**, *311*, 891–907.
(10) North, B. *J. Mol. Biol.* **2006**, *359*, 930–9.
(11) MacKenzie, K. R. *Curr. Opin. Struct. Biol.* **2008**, *18*, 412–9.
(12) Barth, P. *Curr. Opin. Struct. Biol.* **2007**, *17*, 460–6.
(13) Russ, W. P. *J. Mol. Biol.* **2000**, *296*, 911–9.
(14) Wagschal, K. *Protein Sci.* **1999**, *8*, 2312–29.
(15) Choma, C. *Nat. Struct. Biol.* **2000**, *7*, 161–6.
(16) Cristian, L. *Protein Sci.* **2003**, *12*, 1732–40.
(17) Kim, S. *J. Mol. Biol.* **2003**, *329*, 831–40.
(18) Yin, H. *Science* **2007**, *315*, 1817–22.
(19) Barth, P. *Proc. Natl. Acad. Sci. U.S.A.* **2007**, *104*, 15682–7.

JA904625B